TECHNICAL REPORT 2045
July 2014

Road to Silicon Microsphere Fabrication and Mode Coupling

B. N. L. Pascoguin
R. P. Lu
J. M. Kvavle
A. D. Ramirez

SSC Pacific
San Diego, CA 92152-5001

TECHNICAL REPORT 2045
July 2014

Road to Silicon Microsphere Fabrication and Mode Coupling

B. N. L. Pascoguin
R. P. Lu
J. M. Kvavle
A. D. Ramirez

SSC Pacific
San Diego, CA 92152-5001

SSC Pacific
San Diego, California 92152-5001

K. J. Rothenhaus, CAPT, USN
Commanding Officer

C. A. Keeney
Executive Director

ADMINISTRATIVE INFORMATION

The work described in this report was performed for the Office of Naval Research (ONR) by the Advanced Photonics Technologies Branch (Code 55360) of the Enterprise Communications and Networks Division Code 55300), Space and Naval Warfare Systems Center Pacific (SSC Pacific), San Diego, California. This work was funded by ONR's In-house Laboratory Independent Research (ILIR) Program.

Released by
A. J. Ramirez. Head
Advanced Photonic Technologies
Branch

Under authority of
C. Hendrickson, Head
Enterprise Communications
and Networks Division

Kimwipe® is a registered trademark of Kimberly-Clark Corp.

SB

EXECUTIVE SUMMARY

OBJECTIVE

The objective of the optical microsphere resonator project sponsored by the Office of Naval Research was to develop a high-yield process for the formation of single crystal silicon microspheres for optical whispering gallery mode (WGM) resonator applications. The utility of these high Q microspheres was shown in the literature as useful in a myriad of Department of Defense applications such as optical communication filters and switches, modulators and detectors, accelerometers, gyroscopes, and biosensors.

RESULTS

Single crystal silicon microspheres with diameters ranging from 1 to 100 μm were fabricated using the laser ablation technique. Unfortunately, not all particles that were generated were perfectly spherical. This resulted in the need for a two-step filtering process: first to remove the non-spherical particulates, followed by a sorting method for size selection. Uncertainties in whether or not the research team was achieving evanescent coupling in the critical coupling regime with the free standing microspheres led to a test to form a microsphere at the end of an optical fiber using a fusion splicer. With the optical fiber acting as a stem attached to the microsphere it was much easier to control the coupling distance; however, precise control was still difficult due to the Van der Waals forces present between to the insulating materials. The best result achieved was approximately a Q of 1 million, which is about 2 orders of magnitude lower than expected. This could be due to imperfections in the microsphere and maintaining the critical coupling distance.

RECOMMENDATIONS

Disk geometries may be more attractive due to the lower number of modes present and because mode engineering is possible through material modification using a femtosecond laser by generating gratings or photonic crystal patterns on the surface of the disk resonator. Collaboration between SSC Pacific and companies using disk resonators for WGM applications for defense applications could be a viable strategy for future development.

CONTENTS

Figures

INTRODUCTION

The efficiency and methodology of coupling light into microcavities have improved exponentially in the last decade. One such advancement is coupling light onto silicon microspheres. The material, size, and shape of a silicon microsphere are ideal for optical devices because silicon microspheres have a high Q factor. Single crystal silicon microspheres exceed the Q of silicon-dioxide (SiO_2) microspheres due to high refractive index [1]. Silicon microspheres are not the primary material used to fabricate microspheres for optical coupling because current methods used for microsphere fabrication cannot produce single crystal silicon in the 16-µm scale, which is best for current optical technology. Early experiments in silicon microsphere fabrication have been limited to a diameter size of 1 to 5 µm [2] [3].

As described in this report, the pulsed laser ablation method can now produce silicon microspheres that are ideal for optical use. This is a process in which the surface of a silicon substrate is super-heated by a high-power laser until molten and a second laser pulse hits the molten silicon, ejecting micron-sized spherical particles. Furthermore, silicon is naturally abundant, which further enables the large-scale production of optically compatible microspheres.

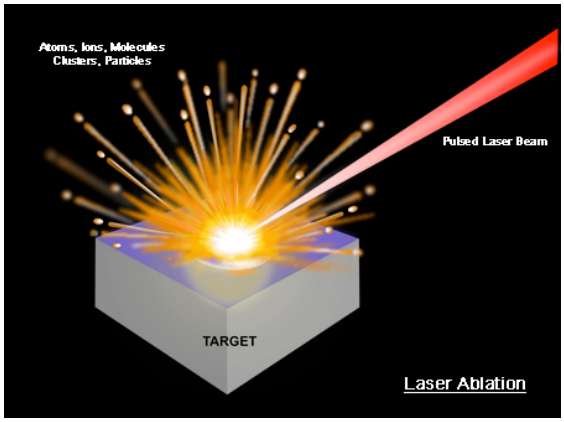

Figure 1. Artistic rendering of the ablation process (courtesy of Applied Spectra [4]).

Coupling light onto microspheres requires delicate techniques such as tapering a single-mode optical fiber to allow coupling from the fiber to the microsphere as well as the fabrication and size sorting of microspheres.

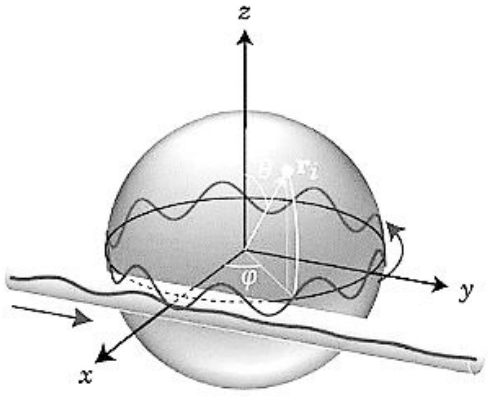

Figure 2. Artistic rendering of light coupled from optical fiber onto a microsphere in whispering gallery mode (courtesy of B. Butkus, Biophotonics International [5]).

BACKGROUND

SILICON MICROSPHERE FABRICATION METHODS

Processes for forming spherical structures exist in nature. The most commonly known example of a microsphere that nature provides is a rain droplet. Rain droplets form a spherical structure while falling in air because of the surface tension in the water molecules taking advantage of this shape, which has the smallest surface area to volume ratio [6].

Thus, a raindrop has a nearly perfect spherical shape as it travels in space. The approach used in this report is to fabricate a single crystal silicon microsphere as inspired by this natural process of raindrop formation. Similarly, as with the microspherical liquid water droplets, ablation of silicon wafer momentarily makes liquid silicon droplets in space, allowing these droplets to form spheres and cool to a solid state before settling onto the silicon wafer surface. This process allows a reproducible large-scale production of silicon microspheres in the 100-μm size scale.

Other methods of fabricating silicon microspheres involve techniques using Chemical Vapor Decomposition (CVD) [3]. One such process, developed by [3], decomposed disiline gas (Si_2H_6) to produce porous, polycrystalline silicon microspheres. Unfortunately, this process of fabricating silicon microspheres restricts the diameter to a maximum of 5 μm. Furthermore, it requires handling hazardous Si_2H_6 gas, which requires using pressure chambers and high-temperature ovens. This method is optimal to produce a high volume of 5-μm silicon colloids for technology such as sunscreen lotion. However, this process is not optimal because research and development purposes require single crystal silicon microspheres.

Another method for fabricating silicon microspheres is to apply laser heating to finely crushed silicon wafers. This method produces single crystal silicon microspheres because the silicon only goes through a physical change, and does not go through any chemical changes [2]. For this fabrication scheme, [2] used machine-pulverized silicon wafers mixed into a solution of alcohol and water. While mixing this solution with a magnetic stirrer, the researchers heated the powdered solution for 30 min by firing a ND:YAG laser beam at 532 nm into the container to melt the silicon powder into microspheres. Reference [2] shows that this method produces single-crystal silicon microspheres up to 2.5 μm in diameter. Although the product is the ideal single crystalline composition for silicon microspheres, the size is still too small for optimal whispering gallery mode (WGM) optical coupling [7] [8].

Q OF THE CAVITY

Coupling light to another medium stores information in the form of resonant frequencies determined by the type of the material, shape, and size of the resonant cavity. How well the resonant frequency couples to its optical structure is the most important characteristic of this medium. When using the Q factor or quality factor of the cavity for the structure, it is possible to define the coupling efficiency to evaluate the aforementioned variables used to design these optically resonant structures.

The Q of the cavity is determined by the width of the resonant peak, more specifically, the width at about 3 dB from the baseline. Equation (1) describes the theoretical definition of the Q of the cavity:

$$Q = 2\pi \frac{Stored\_Eneregy}{Power\_loss}, \tag{1}$$

where Q is the ratio of the stored energy and the power loss.

Another useful equation for describing Q is

$$Q = \frac{\omega_0}{\Delta\omega}, \tag{2}$$

where ω_0 is the center frequency and $\Delta\omega$ is the width of the center frequency [9].

The Q of the cavity can be observed as light begins to excite a particular resonance and the light source is immediately lost. The light continues to propagate as a WGM until dissipated through imperfections in the material. The delta function is the ideal signal for this frequency. However, due to the loss in the medium, the delta function smears. The Q of the system determines the measure of the sharpness of the signal. Silicon microspheres can have a Q value on the order of millions and as high as 10^8, which is why silicon microspheres are good candidates for optical coupling. Reference [10] discusses the theoretical computation.

COUPLED MODE THEORY – A BRIEF SUMMARY

CHARACTERISTIC EQUATION

This explanation begins by discussing the characteristic equation of the microsphere cavity shown in Equations (3) and (4) [1].

$$\left(\eta_s \alpha_s + \frac{\ell}{R_o}\right) j_\ell(k n_s R_o) = k n_s j_{\ell+1}(k n_s R_o)$$
$$\eta_s = \begin{cases} 1, & \text{TE modes} \\ \dfrac{n_s^2}{n_o^2}, & \text{TM modes.} \end{cases} , \tag{3}$$

$$\alpha_s = \sqrt{\beta_\ell^2 - k^2 n_o^2}\,. \tag{4}$$

Space and Naval Warfare Systems Center Pacific (SSC Pacific researchers derived the characteristic equation from Maxwell's equations in the Mie regime, with the boundary condition of electric field and magnetic field vanishing in the radial and azimuthal direction [11]). Therefore, the resulting field is restricted to the polar direction. Using this characteristic equation determines the l-number of the microsphere. The l-number defines the shape of the field that resonates inside the microcavity.

WAVE EQUATION SOLUTION

Figure 3 shows a two-dimensional plot of the wave equation, a visualization of the 1-number.

SPHERICAL

Reference [10] gives the solution to the wave equation in the Mie regime as

$$\begin{aligned} \psi_\phi(\phi) &= \exp[\pm jm\phi] \\ \psi_\theta(\theta) &= \exp\left[-\frac{m}{2}\theta^2\right] H_N(\sqrt{m}\theta), \qquad m \gg 1 \gg \theta \\ \psi_r(r) &= \begin{cases} j_\ell(k n_s r), & r \le R_o \\ j_\ell(k n_s R_o)\exp[-\alpha_s(r - R_o)], & r > R_o \end{cases} \end{aligned} \tag{5}$$

$$\begin{aligned} N_s = \Bigg\{ \sqrt{\frac{\pi}{m}}\, 2^{N-1} N! R_o^2 \Bigg[\left(1 + \frac{1}{\alpha_s R_o}\right) j_\ell^2(k n_s R_o) \\ - j_{\ell-1}(k n_s R_o) j_{\ell+1}(k n_s R_o) \Bigg] \Bigg\}^{-1/2} \end{aligned} \tag{6}$$

$$\alpha_s = \sqrt{\beta_\ell^2 - k^2 n_o^2}, \quad \beta_\ell = \frac{\sqrt{\ell(\ell+1)}}{R_o}$$
$$N = \ell - m, \qquad k = \frac{2\pi}{\lambda}$$

where the scalar field is defined as

$$\Psi_{\ell,m,n}(r, \theta, \phi) = N_s \psi_r(r) \psi_\theta(\theta) \psi_\phi(\phi)\,. \tag{7}$$

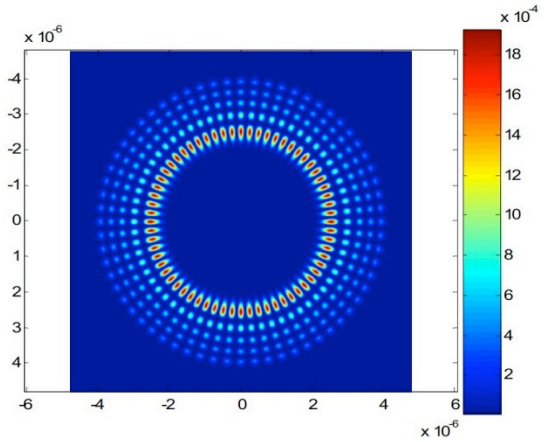

Figure 3. N = 4, l = 32, m = 32.

In Figure 3, there are 32 maxima around the sphere and 4 maxima radially. Therefore, the mode number N and l are the number of maxima allowed in the radial and azimuthal direction.

This report does not provide a complete description of the theory of coupling light. Many of the computations come from [10] and only serve as a brief introduction to support the procedure described in the next section.

FABRICATION

This section discusses reproducible methods for fabricating consistent 2- to 3-μm tapered fibers, silica microspheres, and silicon microspheres.

TAPERED FIBER FABRICATION

The procedure for fabrication first requires stripping off the jacket and buffer from a short section at the end of an optical fiber, followed by the slow heating and stretching of this exposed area until the taper is the desired diameter.

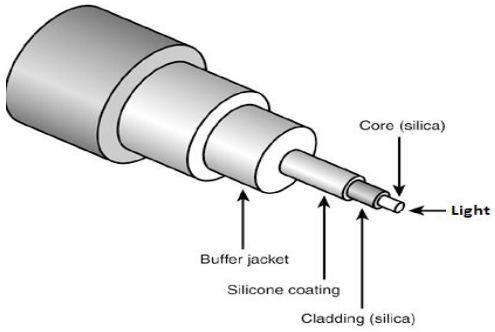

Figure 4. Layers of an optical fiber.

In the following section, the technique used for the tapers in this report are discussed in detail, beginning with the mechanical set-up, followed by the concept behind the program written, and finally the resulting tapered fiber.

FIBER-OPTIC TAPERING SET-UP

Researchers used the fiber-optic tapering set-up shown in Figures 5 and 6 to create tapered fiber. This tapering set-up consisted of two motorized clamps and a torch.

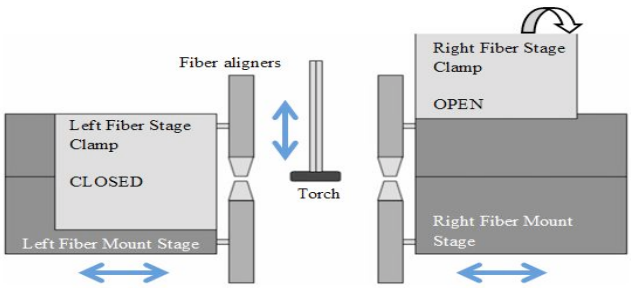

Figure 5. Fiber-optic tapering set-up (top view). The left and right boxes are the clamp and the stages that stretch the fiber. The center is the torch.

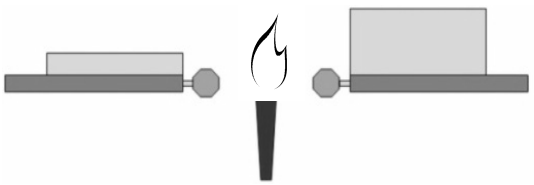

Figure 6. Fiber-optic tapering set-up (side view). The left and right boxes are the clamp and the stages that stretch the fiber. The center is the torch.

Figure 5 shows the top view of the fiber-optic tapering machine. The two stages on the left and the right are motorized clamps that pull the fiber apart as the gas torch, which a separate motor controls, moves slowly vertically while the two clamp stages move laterally. Figure 6 shows the side view of the machine.

The Torch

Butane and oxygen with a 60/20 ratio fueled the torch. Other combinations extinguish the flame. In addition, after switching on the gas lines and setting the gas gauge to 60/20, one must wait 2 to 5 min before igniting the torch with a lighter to kindle the flame successfully. The unsettling of the torch gas and small perturbations, such as breathing or the torch movement, caused some gas flow distortion on the tip of the torch, which made ignition difficult.

Fiber-Optic Tapering Alignment

Researchers placed a small fiber about 5 to 6 inches between the two clamp stages. After turning on the stages and the computer, the “U500” controlled the stages and the torch position. First, with the single mode fiber (SMF) clamped in place, researchers manually moved the torch such that the SMF was directly above it as shown in Figure 7. The distance between the preset location and the set torch z-axis position was recorded for automation. This distance can be used in the future when designing a fiber-stretching program.

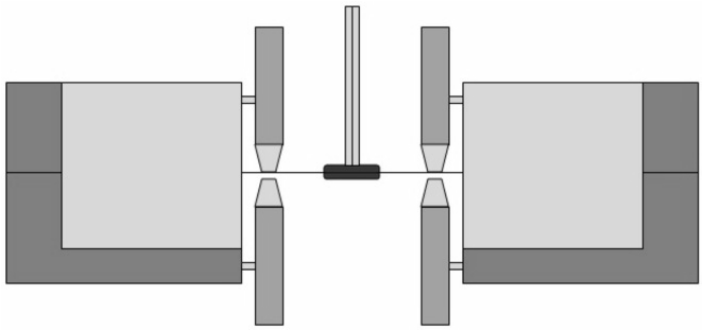

Figure 7. SMF loading alignment.

Figure 8 shows the fiber in the aligned position. The three main components of the fiber-optic tapering set-up are the two clamp stages and the torch. The next section discusses how the fiber was loaded on the tapering set-up.

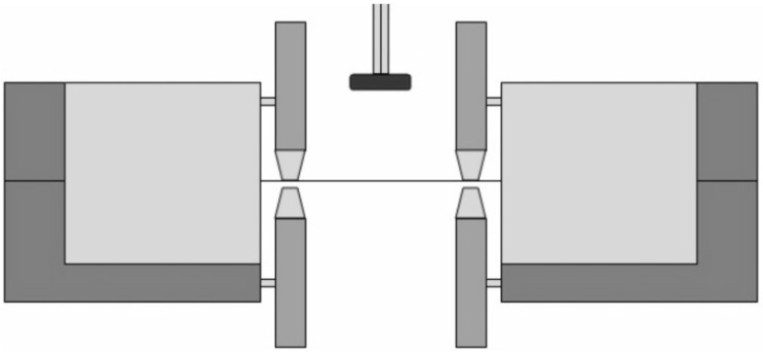

Figure 8. Torch with a known displacement from the fiber.

FIBER PREPARATION AND LOADING

The type of fiber used in this report was a SMF-28 with a core diameter of 8.2 μm. The length of fiber that was tapered was about 1 m. Researchers used a fiber stripper to strip a quarter of an inch of cladding in the middle of the 1-m fiber. They used a Kim-wipe® and an ample amount of isopropanol, and cleaned the residue from the cladding on the fiber by applying a small amount of pressure and pinching the fiber between the wet Kim-wipe®. Using the aligned tapering set-up, the stripped fiber was loaded on the clamp stage and secured by tightening the clamps. Alignment is a crucial element of this process. If there is any misalignment, the tapered fiber may crack and break because of the shear tension. A program was written to automate the tapering process controlling the torch and the stages to produce tapers of consistent diameter and length. The steps of the program are described in the following sections.

PRE-STRETCHING

In the pre-stretching phase, the two clamp stages were moved in phase to place the stripped fiber into the pre-heat phase for further cleaning as shown in Figure 10. Figure 9 shows the schematic before executing the program. The pre-heating removes the excess debris left on the cladding strip by burning off the buffer and jacket residue.

Figures 11 and 12 show the motion of the clamp stages moving in phase while heat cleaning the stripped portion of the fiber. After the pre-heating phase, the program returned the torch and the fiber to the alignment position. The program has a 2-sec wait period at this stage to soften the cladding and core further so the fiber would be less likely to fracture when stretched as shown in Figure 13. Figures 14 and 15 show the right and left stages moving individually to stretch the fiber one side at a time. This step controls the taper diameter by augmenting the number of stretches in the program. At the end of the stretching, an additional post-heating process begins. The post-heating phase added extra gravitational sag to the tapered fiber. If the fiber was not post-heated, the tapered fiber would have cooled at a higher tension because the stretching procedure would make removal of the tapered fiber far more difficult as it would have a high tendency to break.

These steps are redefined in the step-by-step diagrams in Figures 9 through 16.

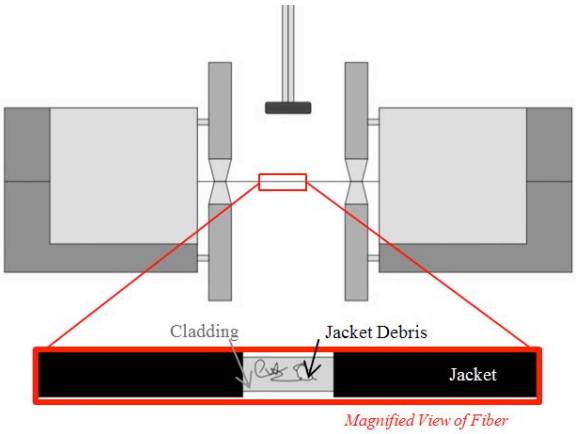

Figure 9. The set-up before pre-heating starts. Note the close-up of the fiber still shows jacket debris left after the acetone clean.

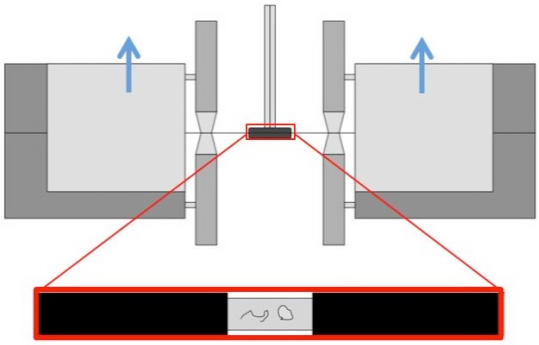

Figure 10. The torch lines up with the fiber.

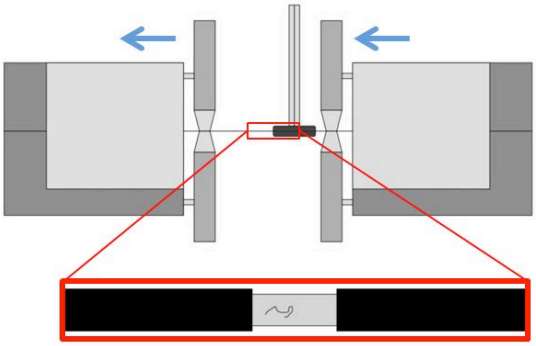

Figure 11. The clamp stage moves in phase to the left to clean excess debris.

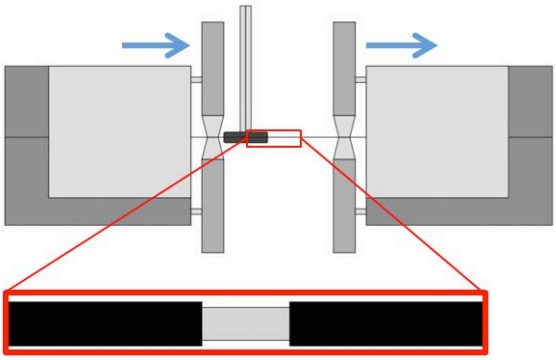

Figure 12. The clamp stage moves in phase to the right to clean excess debris.

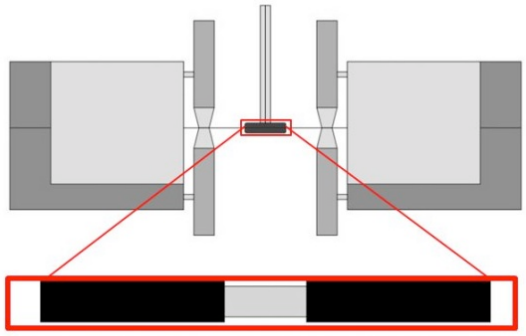

Figure 13. Re-center the torch and pause for 2 sec.

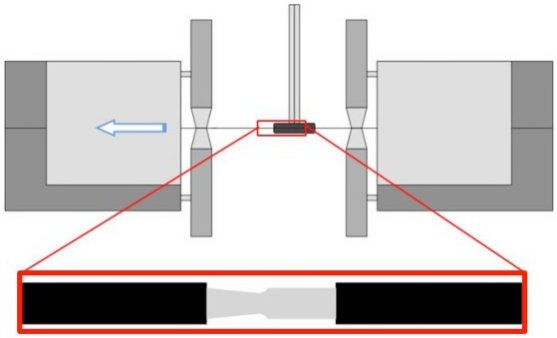

Figure 14. The clamp stages move independently.

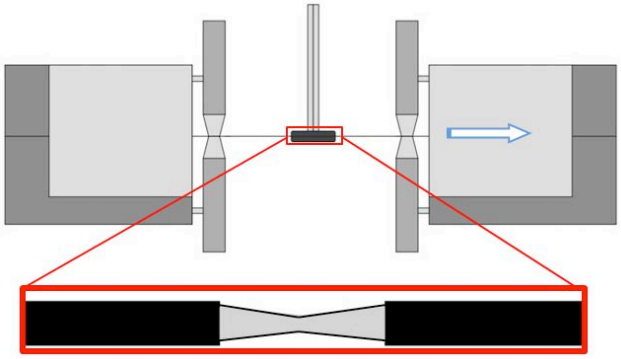

Figure 15. The clamp stages move individually one at a time; this repeats until the desired amount of stretching is complete and then pauses again for 5 sec.

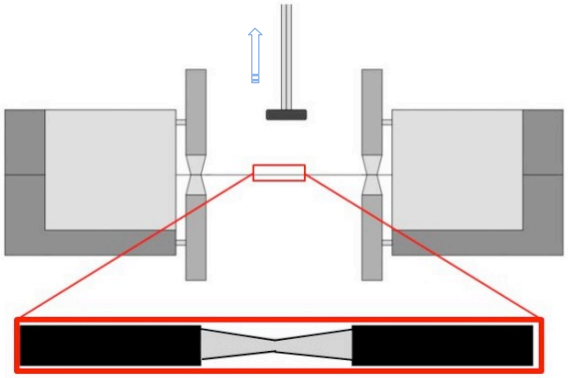

Figure 16. The torch retreats back to the reset position and is now ready for the next tapering.

TAPER REMOVAL

As expressed in the previous section, removing the taper from the fiber-optic tapering set-up was the most difficult step in the fiber tapering process. Even a small twitch could have broken the taper. The macroscopic process for removing the tapered fiber is very simple, unscrew the two clamps and take the fiber out; however, the mechanics for keeping the taper intact requires more care.

Using a pair of tweezers to hold one end of the fiber towards the torch and carefully unscrewing only one side of the clamps helped. Using tweezers prevented the fiber from moving as it was unscrewed. After freeing the taper from the clamp, researchers gently rested the taper over the clamp, and then re-screwed the clamp to the closed position. They repeated this procedure on the other side.

After freeing the fiber from the clamps, researchers formed the clamp into a U-shape. They used a square glass slide to tape the tapered fiber on the glass slide and fix it into position as shown in Figure 17.

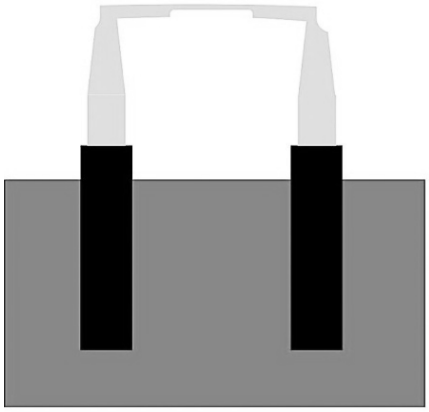

Figure 17. Tapered fiber on a glass slide.

The program written for this report consistently produced a 2- to 3-µm taper. Figure 18 shows a 3-µm taper next to a 100-µm-diameter microsphere.

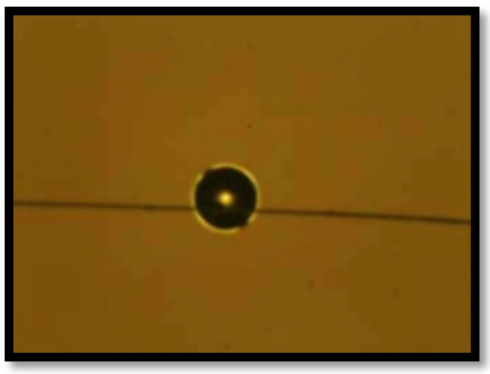

Figure 18. 100-µm-diameter silica next to a 3-µm-diameter taper.

The next section will discuss the methods that were used for fabricating microspheres.

MICROSPHERE FABRICATION

This section discusses two methods of fabricating a microsphere. The two types of microspheres fabricated were silica and silicon. The goal of the next experiment described in this report was to fabricate a silica microsphere.

Microsphere-Tipped SMF-28 Optical Fiber via Splicer

Fabricating silica microspheres required the exposure of a section of the cladding by stripping the jacket from the optical fiber, heating it, and lastly melting one end using a fusion splicer, which led to the formation of a microsphere. The next section describes how to control the size and go into more detail on the fabrication of silica microsphere.

Silica Microsphere Size Control

Again, researchers stripped about an inch of the cladding off the end of the fiber as shown in Figure 19. Using the same torch used to create a tapered fiber, they heated the fiber above the flame and gently stretched it to reduce the diameter further as shown in Figure 20.

By creating small dimples in the cladding through holding the upper portion of the fiber over the flame as shown in Figures 21 and 22, they created a low-high-low shape. After achieving this shape, they heated one side of the dimple, separating the fiber into two pieces. The resulting fiber should look like Figure 23.

Figure 19. Fiber with cladding stripped off.

Figure 20. Stretched fiber.

Figure 21. Creating the right dimple.

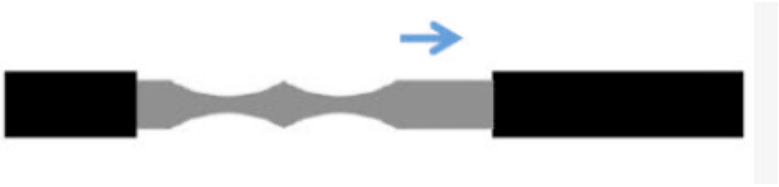

Figure 22. Creating the left dimple.

Figure 23. Low-high-low profile.

Researchers used an older model fusion splicer to manually arc the tip of the dimple to create a spherical shape by arcing the tip as shown in Figures 24 through 28. The result of the initial arc was not quite spherical but rather only somewhat round as shown in Figure 26. Figure 27 shows that the fiber must be adjusted upwards to apply an arc to the tip of the quasi-sphere. After multiple arcs, the shape of the tip should look like a sphere shown in Figure 28.

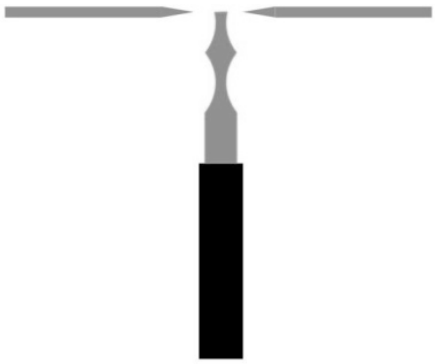

Figure 24. Position of the fiber on the fusion splicer.

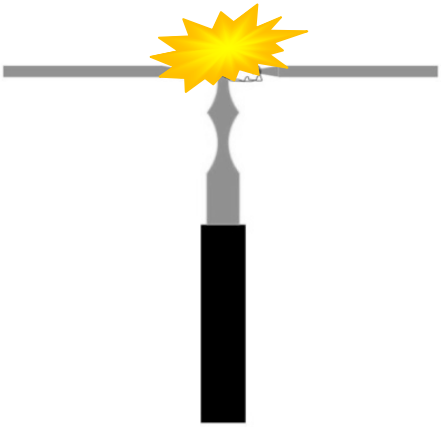

Figure 25. Fusion splicer arcs fiber.

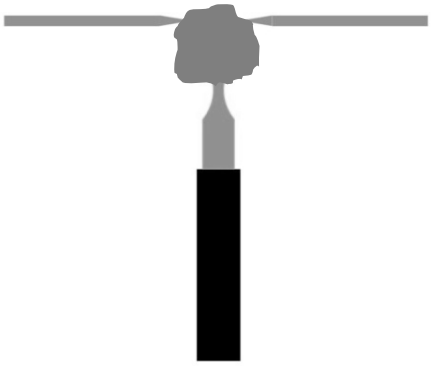

Figure 26. Initial arc result.

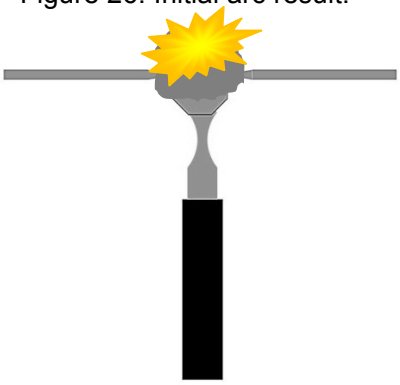

Figure 27. Arcing repeated to achieve a spherical shape.

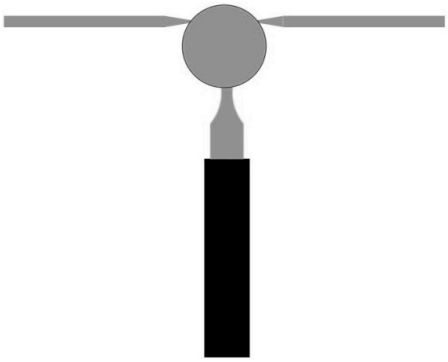

Figure 28. Final product.

The typical amount of arc repetition was about 3 to 7 times for a 200-µm-diameter sphere. To make a smaller microsphere, it is necessary to decrease the low-high-low taper shown in Figure 20 and arc the fiber less than 5 times. Figure 29 is one of the 200-µm-diameter microspheres that was made by using the technique detailed in this section.

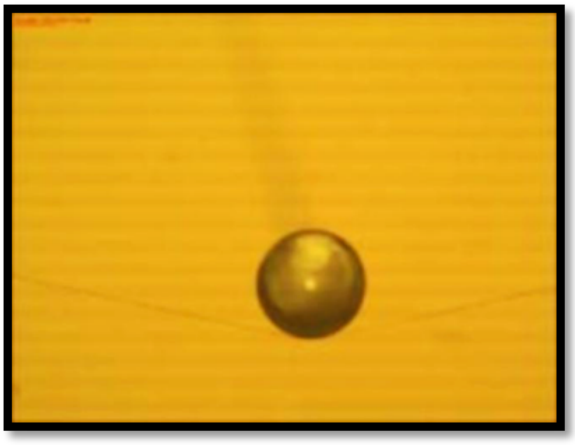

Figure 29. A fabricated silica microsphere with stem faintly visible.

The next section shows how to fabricate and collect silicon microspheres using laser ablation and light probing.

TWO-LENS SILICON MICROSPHERE FABRICATION

The two-lens system shapes the spot size of the beam at the focal length to a small point. The set-up used a spherical lens of a focal length of about half a meter followed by a cylindrical lens with a focal length of 15 cm.

Without the spherical lens, the cylindrical lens had a focus of a 4-inch line profile. With the spherical lens, the cylindrical lens had a focused spot size of less than an inch. By shrinking the spot size of the spherical lens, the energy density of the laser beam over that spot surface area increased.

ABLATION

With the silicon wafer as the target, the excimer laser (308 nm) was set to 400 mJ and 50 Hz for optimized ablation. Figure 30 shows the optical system set-up.

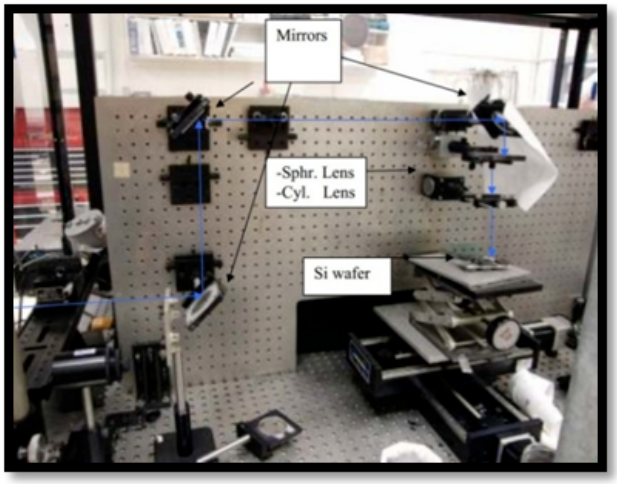

Figure 30. Optical set-up.

As shown in Figure 30, researchers mounted the silicon wafer target on a z-translation stage. The silicon wafer could now be positioned in and out of the focus. This set-up was necessary because as the excimer laser ablated the wafer, the silicon surface target was no longer in focus because of the removal of the surface material.

SILICON WAFER ABLATION IN MAGNETIC FIELD

Assuming that ablated silicon possesses some charge, the ablated debris will be subject to motion under a magnetic field. However, the influence of the magnetic field may have only been for a moment because of the debris' short time in the semi-plasma state.

Semi-Plasma State

When the silicon wafer surface was ablated, the debris ejected from the surface was molten due to the short-duration, high-energy laser pulse. Because of the short time in the laser pulse, the debris did not fully reach a plasma state and remained mostly solid. Knowing that plasmas are a sea of charge, presumably at this "semi-plasma state," the glowing debris would be quasi-charged and may be subject to move directionally under the influence of a magnetic field.

Figures 31 and 32 show the actual and the schematic visualization of the magnetic sorting of the semi-plasma state of the ablated silicon particles.

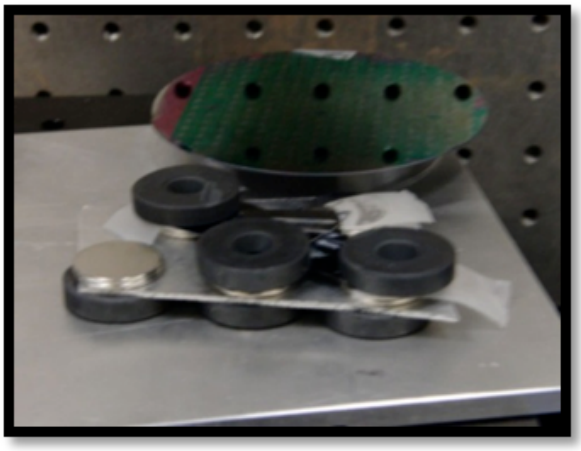

Figure 31. Image of silicon wafer target under a magnetic field and an adjacent collection wafer.

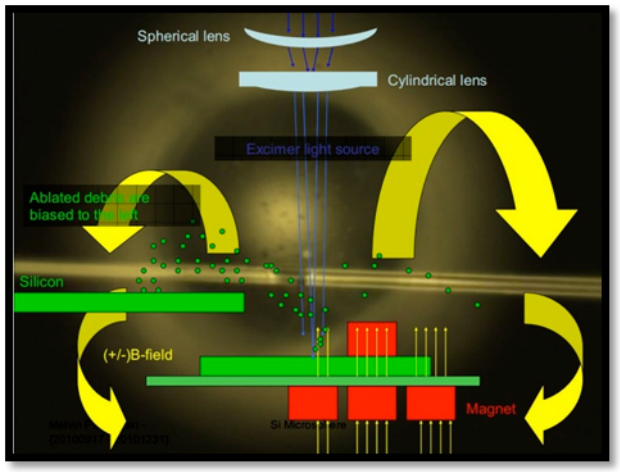

Figure 32. Magnetic sorting schematic.

Figure 31 shows that one side of the sample has a stronger magnetic field than the other side. This magnetic gradient was the key to sorting the particles. If T_A is considered as the time of the ablated silicon in the semi-plasma state, then at least a quarter of that time will be spent shooting up. Because charged particles follow the field lines of the magnetic field [7] for the duration of T_A, the ablated materials were biased to move along lower magnetic field lines where the debris was collected at their resting location. However, the initial velocity and direction of the particulate also dictates where the debris will ultimately land. Figure 33 shows the collected debris after ablation.

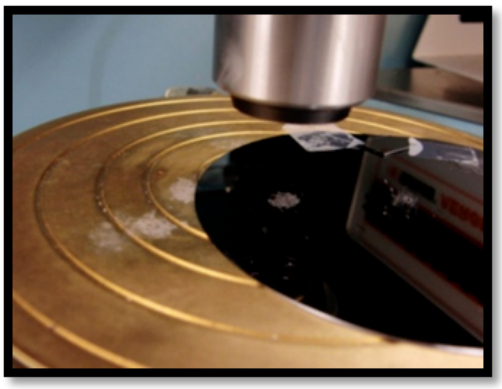

Figure 33. Collected silicon ablated debris.

SILICON MICROSPHERE SORTING

Once the debris from the silicon wafer ablation was collected, the next step was to separate the microspheres from the silicon debris.

In this step, each microsphere must be sorted out of the debris individually. Researchers used a tiny 20-µm-diameter probe attached on the tip of a pin here. Through some image processing and programmed probe mechanics, it may be possible to automate this process in the future.

Under a microscope, researchers identified a clean spot on the wafer to collect the silicon microsphere. From the pile of debris, they used the probe to sweep over the surface to look for circular objects. Figure 34 shows the actual process of the silicon selection process.

After spotting and isolating the silicon microsphere, researchers statically picked it up with the probe and moved it onto a designated clean spot on the wafer as shown in Figure 35.

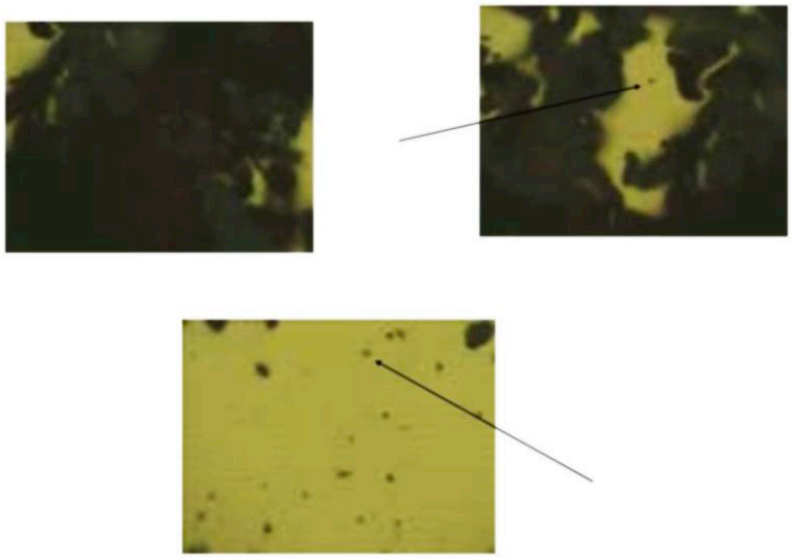

Figure 34. Top left shows the pile of debris. Top right shows the 10-μm sphere spotted. Bottom shows the silicon microsphere isolated.

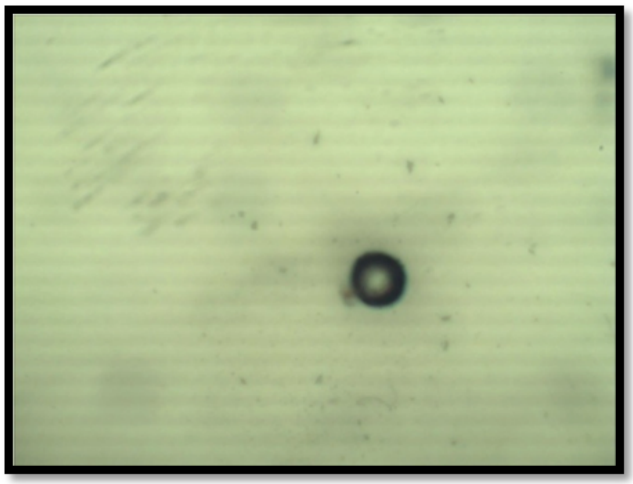

Figure 35. 14-μm silicon microsphere.

Size Limitation

The size of the collected microsphere ranges from 5 to 15 μm. The pressure may have an effect on fabricating these spheres because of intermolecular forces as described by the Van der Waals equation in statistical mechanics.

MICROSPHERE COUPLING (EXPERIMENTAL)

This section discusses the methods and techniques used in this report to couple a microsphere onto a taper. The concept for how to couple light is simple. Place the microsphere next to the taper. Figure 36 shows the experimental set-up used for the coupling of the tapered fiber and the microsphere. A baseline signal was recorded in the absence of a microsphere and compared with the signal recorded when a microsphere was present. Rsearchers also used a polarizer to maximize the coupling signal.

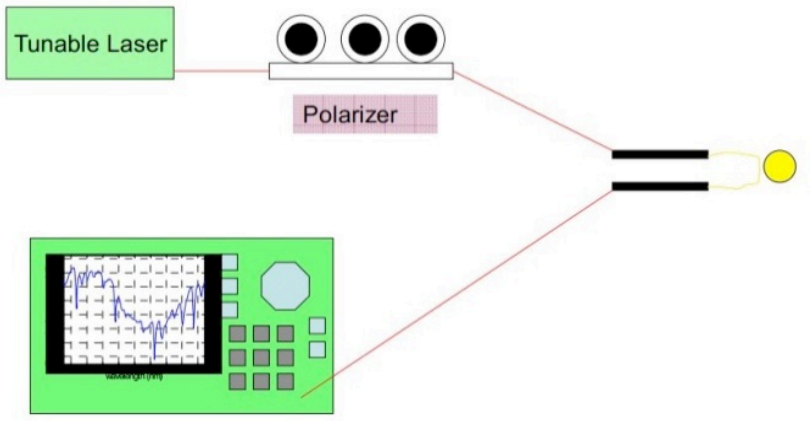

Figure 36. Coupling set-up.

COUPLING TECHNIQUE USED

Coupling with the fabricated silica microsphere was straightforward, as researchers had attached it to a stem for mounting onto a holder. This set-up helps the microsphere remain steady in mid-air when the taper is brought close enough for coupling light. Figure 37 shows the actual coupling of the fabricated silica microsphere. The arrow indicates the rod/stem that is out of focus.

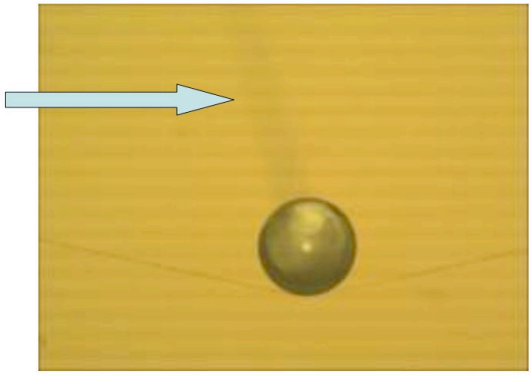

Figure 37. Fabricated silica microsphere coupling.

Figure 38 shows the infrared photo of a silica microsphere coupling onto a tapered fiber. Note how the right side of the tapered fiber is significantly brighter than the left side and that the microsphere is glowing bright.

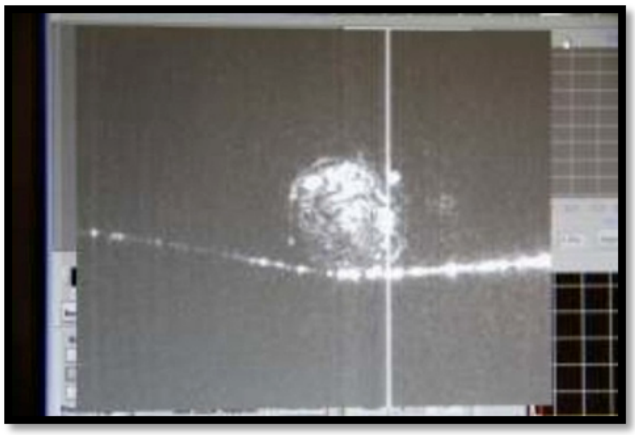

Figure 38. Infrared image of coupling.

Silica Microsphere Coupling

The next step, however, does not use a stem, but rather just a freestanding sphere. While coupling with the fabricated silica, a strong electro-static attraction exists between the taper and the fabricated microsphere. Initially, researchers used an ionizing fan to diminish the static to optimize the position of the taper onto the microsphere. However, with the freestanding silica microsphere, researchers could use the static force between the microsphere and the taper as a tool for attaching microspheres onto the taper without any external object disturbing the whispering gallery mode around the microsphere.

120-µm and 10-µm Coupling

Figure 39 shows the static attachment of the 100-µm (on top) and 10-µm (on bottom) microsphere onto a 3-µm taper. The right side is the same image at 125x magnification.

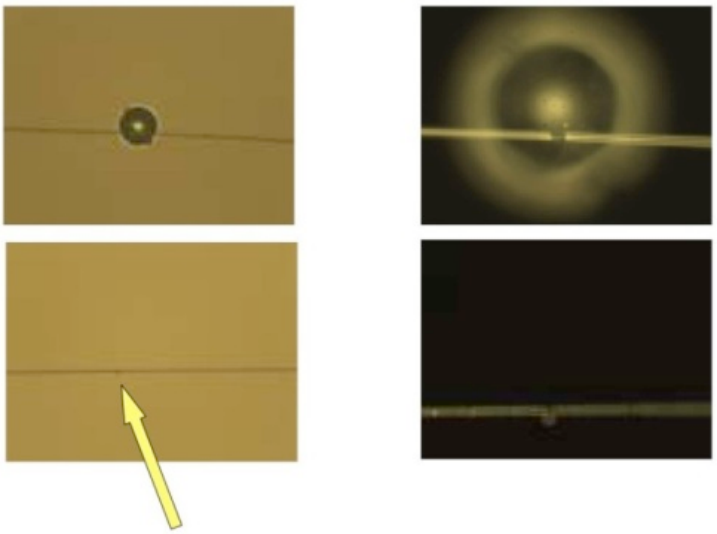

Figure 39. Static coupling of silica microsphere.

Figure 40 shows the coupling result of the 100- and 10-µm microspheres and the corresponding theoretical free spectral range of the coupling.

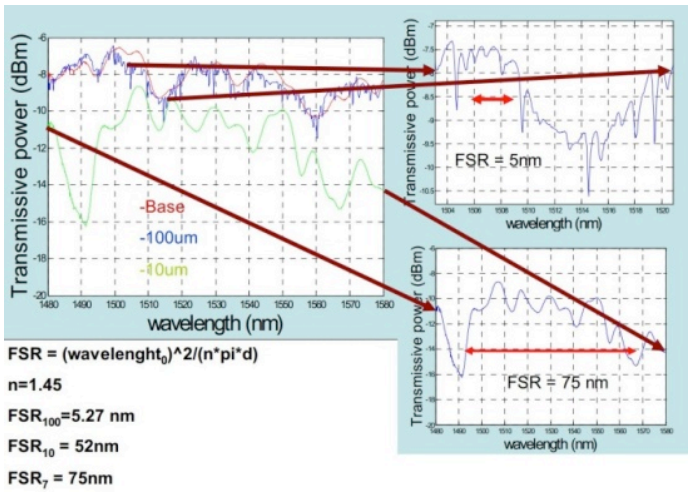

Figure 40. Silica coupling result from optical spectrum analyzer.

Note that the predicted value is close to the experimental value, which is a good indication of coupling. In addition, the resonance peak shifts as the polarizer is moved, which is another sign of coupling.

COUPLING WITH SILICON MICROSPHERE

Coupling a silicon microsphere is the same as the silica microsphere coupling. Figure 41 shows a 13-µm fabricated silicon microsphere coupling.

Figure 41. 13-µm silicon microsphere coupling.

Figure 42 shows the comparison of the optical spectrum analyzer signal before and after researchers statically attached the silicon microsphere to the tapered fiber.

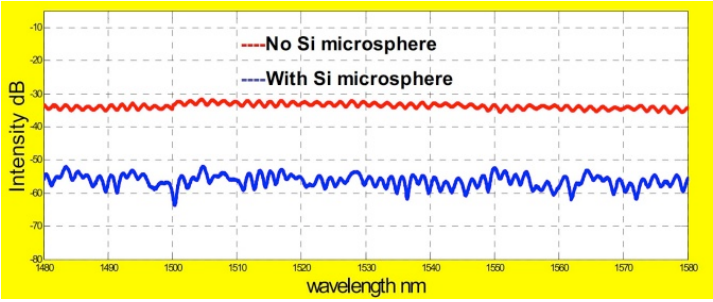

Figure 42. Comparison of the base signal vs. silicon microsphere coupling.

Although Figure 42 does not show the resonant frequency clearly, Figure 43 shows the distinction of the resonant peaks of the coupling.

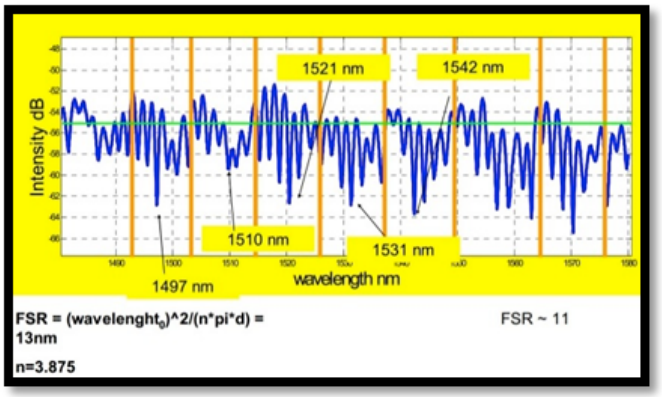

Figure 43. Zoomed-in image of the silicon microsphere coupling.

Figure 44 shows the same signal as Figure 43 but with a different polarization and the resonant shifted as the polarization was slightly changed.

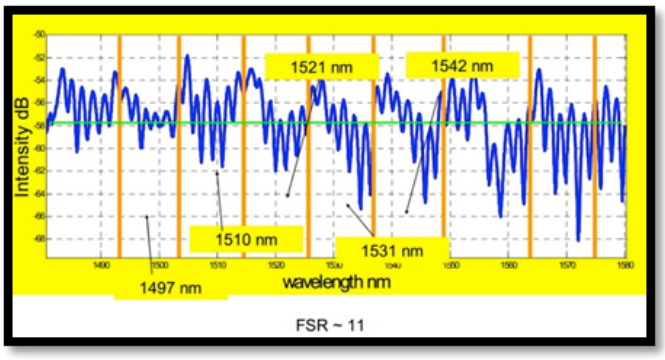

Figure 44. Different polarization.

SILICON MICROSPHERE FABRICATION SUMMARY

Methods Attempted

Plasma Torch

While waiting for the gas for the laser, a plasma torch was used to ablate the silicon wafer. But this didn't produce any microspheres.

Single Pulse Ablation

The problem with this method is that the microsphere is less than a micron and the microsphere is melted to the wafer.

Chemical Coating

This method is too messy.

Water

Water cracks the silicon wafer if no damper is placed around the ablated area.

Glycerol

Glycerol did not work.

Immobilized Particle Arrays (IPAs)

IPAs did not work.

Butane Torch + Excimer Ablation

The torch only heats the wafer, causing it to be brittle, and once ablated, the wafer simply cracks.

Crushed Silicon

This method is too messy. Crushed silicon is dispersed all over the place and no microspheres were produced.

Methods Not Attempted

Pre-pulse Method

Excimer + Excimer

CO2 + Excimer

Disiline Gas 40

CONCLUSION

The experimental free spectral range (FSR) obtained was within 15 percent difference in comparison to the simulation models. The challenge of coupling is the manipulation of the small optical resonator into position. Getting the distance between the tapered fiber waveguide and the microsphere correct such that they lie in the critical coupling region to achieve perfect evanescent field coupling was difficult. Over-coupling tends to occur because static electricity causes the tapered fiber to stick to the microsphere when the two objects approach one another.

Future studies include functionalizing the microsphere surface for ultrasensitive biochemical sensors through the detection of resonant frequency shifts. Theoretical studies have shown that label-free single molecule detection should be feasible in principle because of the high Q properties of the optical resonator. Disk geometries may be more attractive due to the lower number of modes present and because mode engineering is possible through material modification using a femtosecond laser by generating gratings or photonic crystal patterns on the surface of the disk resonator.

REFERENCES

[1] E. Xifré-Pérez, J. D. Domenech, R. Fenollosa, P. Muñoz, J. Capmany, and F. Meseguer. 2011. "All Silicon Waveguide Spherical Microcavity Coupler Device," *Optics Express 19*:3185–3192.

[2] X. Li, A. Pyatenko, Y. Shimizu, H. Wang, K. Koga, and N. Koshizaki. 2011. "Fabrication of Crystalline Silicon Spheres by Selective Laser Heating in Liquid Medium," *Langmuir* 27(8):5076–5080.

[3] Roberto Fenollosa, Fernando Ramiro-Manzano, Michal Tymczenko and Francisco Meseguer J. Mater. 2010. "Porous Silicon Microspheres: Synthesis, Characterization and Application to Photonic Microcavities," *Journal of Materials Chemistry 20*:5210–5214.

[4] Photograph online at http://www.appliedspectra.com/technology/laser-ablation.html

[5] Photograph online at B. Butkus. "Silica Microspheres Enable Sensitive DNA Detection." October 2003. Biophotonics International. http://www.rowland.org/rjf/vollmer/images/biophotonics.pdf

[6] James E. McDonald. 1954. "The Shape and Aerodynamics of Large Raindrops," *Journal of Meteorology 11*:478–494.

[7] M. J. Humphrey, E. Dale, A. T. Rosenberger, and D. K. Bandy. 2007. "Calculation of Optimal Fiber Radius and Wispering-gallery Mode Spectra for a Fiber-coupled Microsphere," *Optics Communications 271*:124–131.

[8] H. Agha Imad, Yoshitomo Okawachi, and Alexander L. Gaeta. 2009. "Theoretical and Experimental Investigation of Broadband Cascaded Four-wave Mixing in High-Q Microspheres," *Optics Express 17*:16209–16215.

[9] J. D. Jackson. 1998. *Classical Electrodynamics*. Third Edition. John Wiley & Sons. New York, NY.

[10] Brent E. Little, J.-P. Laine, Hermann A. Haus, and Life Fellow. 1999. "Analytic Theory of Coupling from Tapered Fibers and Half-Blocks into Microsphere Resonators," *Journal of Lightwave Technology 17(4)*:704–715.

[11] I. H. Agha, J. E. Sharping, M. A. Foster, and A. L. Gaeta. "Optimal Sizes of Silica Microspheres for Linear and Nonlinear Optical Interactions," *Applied Physics B: Lasers and Optics 83(2)*:303–309. DOI: 10.1007/s00340-006-2155-8.

[12] F. F. Chen. 1983. *Introduction to Plasma Physics and Controlled Fusion.* Volume 1. Plenum Press, New York, NY.

REPORT DOCUMENTATION PAGE

Form Approved
OMB No. 0704-01-0188

PLEASE DO NOT RETURN YOUR FORM TO THE ABOVE ADDRESS.

1. REPORT DATE *(DD-MM-YYYY)*	2. REPORT TYPE	3. DATES COVERED *(From - To)*
July 2014	Final	

4. TITLE AND SUBTITLE

Road to Silicon Microsphere Fabrication and Mode Coupling

5a. CONTRACT NUMBER

5b. GRANT NUMBER

5c. PROGRAM ELEMENT NUMBER

6. AUTHORS

B. N. L. Pascoguin
R. P. Lu
J. M. Kvavle
A. D. Ramirez

5d. PROJECT NUMBER

5e. TASK NUMBER

5f. WORK UNIT NUMBER

7. PERFORMING ORGANIZATION NAME(S) AND ADDRESS(ES)

SSC Pacific, 53560 Hull Street, San Diego, CA 92152–5001

8. PERFORMING ORGANIZATION REPORT NUMBER

TR 2045

9. SPONSORING/MONITORING AGENCY NAME(S) AND ADDRESS(ES)

Office of Naval Research
800 North Quincy Street
Arlington, VA 22217–5000

10. SPONSOR/MONITOR'S ACRONYM(S)

11. SPONSOR/MONITOR'S REPORT NUMBER(S)

ONR

12. DISTRIBUTION/AVAILABILITY STATEMENT

Approved for public release.

13. SUPPLEMENTARY NOTES

14. ABSTRACT

As described in this report, silicon microspheres that are ideal for optical use can now be produced through pulsed laser ablation. This is a process in which the surface of a silicon substrate is super-heated by a high-power laser until molten and a second laser pulse hits the molten silicon, ejecting micron-sized spherical particles. Furthermore, silicon is naturally abundant, which further enables the large-scale production of optically compatible microspheres.

The experimental free spectral range (FSR) obtained was within 15 percent difference in comparison to the simulation models. The challenge of coupling is the manipulation of the small optical resonator into position. getting the distance between the tapered fiber waveguide and the microsphere correct such that they lie in the critical coupling region to achieve perfect evanescent field coupling was difficult. Over-coupling tends to occur because static electricity causes the tapered fiber to stick to the microsphere when the two objects approach one another.

Future studies include functionalizing the microsphere surface for ultrasensitive biochemical sensors through the detection of resonant frequency shifts. Theoretical studies have shown that label-free single molecule detection should be feasible in principle due to the high Q properties of the optical resonator. Disk geometries may be more attractive because of the lower number of modes present and mode engineering is possible through the material modification using a femtosecond laser by generating gratings or photonic crystal patterns on the surface of the disk resonator.

15. SUBJECT TERMS

silicon microsphere fabrication
silica microsphere fabrication
whispering gallery mode
optical coupling
microsphere coupling
fiber-optic tapering
ablation process

16. SECURITY CLASSIFICATION OF:			17. LIMITATION OF ABSTRACT	18. NUMBER OF PAGES	19a. NAME OF RESPONSIBLE PERSON
a. REPORT	b. ABSTRACT	c. THIS PAGE			R. P. Lu
U	U	U	U	34	19B. TELEPHONE NUMBER *(Include area code)* (619) 767-4172

INITIAL DISTRIBUTION

84300	Library	(2)
85300	Archive/Stock	(1)
55360	B. M. L. Pascoguin	(1)
55360	R. P. Lu	(17)
55360	J. M. Kvavle	(1)
55360	A. D. Ramirez	(1)

Defense Technical Information Center
Fort Belvoir, VA 22060–6218 (1)

Approved for public release.

SSC Pacific
San Diego, CA 92152-5001